2—5

Natural Image Correction by Iterative Linear Projection onto Eigenspaces

Fumihiko Sakaue   Takeshi Shakunaga *
Department of Information Technology, Okayama University

Abstract

The present paper reports an image correction method that is based on iterative projection onto eigenspaces. The fundamental method proposed in Shakunaga and Sakaue[11] and involves iterative analysis of relative residual and projection. The present paper refines the projection method by solving linear equations while taking noise ratio into account. The refinement improves both the efficiency and robustness of the projection. Experimental results indicate that the proposed method works well for various kinds of noise, including shadows, reflections and occlusions. The proposed method can be applied to a wide variety of computer vision problems, which include object/face recognition and image-based rendering.

1 Introduction

In object/face recognition, eigenspaces are used with various kinds of discrimination criteria [1, 2, 3, 4, 6, 8, 9, 10, 12, 13, 14]. Eigenspaces are also effective for image based rendering with varying lighting conditions [7, 5]. While eigenspaces are usually constructed by PCA, eigenspaces can also be constructed from original images based on the photometric SVD algorithm [15]. However, the eigenspace should be carefully constructed if the original images include noises such as shadows, reflections or occlusions. For this problem, we have proposed a RANSAC approach [5] to a 3-d eigenspace construction for Lambertian objects in order to realize photometric image-based rendering.

In object/face recognition, however, we encounter another problem. That is, eigenspace-based methods always assume that a projection is made correctly from a given image. When projections are made from images containing a lot of noise, the projections are often suffer from effects of the noise. In order to solve this problem, Shakunaga and Sakaue[11] proposed an image correction method based on the iterative projection of images onto eigenspaces, in which noise detection using the relative residual is essential. The present paper refines the method in both efficiency and robustness.

2 Notations and Basic Relations

2.1 Normalized Image Space (NIS)

The Normalized Image Space (NIS) was proposed by Shakunaga and Shigenari[10]. Let $\mathbf{X}$ denote an n-dimensional image, and $\mathbf{1}$ denote an n-dimensional vector of which any element is 1. The normalized image

*Address: Okayama-shi, Okayama 700-8530, Japan. E-mail: {sakaue,shaku}@chino.it.okayama-u.ac.jp

$\mathbf{x}$ of an original image $\mathbf{X}$ is defined as $\mathbf{x} = \mathbf{X}/\mathbf{1}^T\mathbf{X}$. After normalization, $\mathbf{x}$ is normalized in the sense that $\mathbf{1}^T\mathbf{x} = 1$. The NIS is closed to any averaging operation.

2.2 Projection and Residual in NIS

Let $\mathbf{x}^*$ denote a projection of n-dimensional vector $\mathbf{x}$ to an m-dimensional eigenspace. That is,

$$\mathbf{x}^* = \Phi_m^T(\mathbf{x} - \overline{\mathbf{x}}) \tag{1}$$

where Φ_m consists of $m(m < n)$ orthogonal bases of the eigenspace, and $\overline{\mathbf{x}}$ denotes a center of the eigenspace. Let $\mathbf{x}^\sharp$ denote a residual of the projection,

$$\mathbf{x}^\sharp = \mathbf{x} - \overline{\mathbf{x}} - \Phi_m\mathbf{x}^*. \tag{2}$$

2.3 Effect of Noise on Projection/Residual

When an image $\mathbf{X}$ is a weighed sum of a signal image $\mathbf{X}_S$ and a noise image $\mathbf{X}_N$, the image $\mathbf{X}$ is normalized to

$$\mathbf{x} = (1 - \alpha)\mathbf{x}_S + \alpha\mathbf{x}_N \tag{3}$$

where $\mathbf{x}_N = \mathbf{X}_N/\mathbf{1}^T\mathbf{X}_N$, $\mathbf{x}_S = \mathbf{X}_S/\mathbf{1}^T\mathbf{X}_S$ and α is a value called the noise ratio, which is denoted by

$$\alpha = \mathbf{1}^T\mathbf{X}_N/\mathbf{1}^T\mathbf{X}. \tag{4}$$

Then, $\mathbf{x}^*$ and $\mathbf{x}^\sharp$ are given as

$$\mathbf{x}^* = (1 - \alpha)\mathbf{x}_S^* + \alpha\mathbf{x}_N^* \tag{5}$$

$$\mathbf{x}^\sharp = \alpha(\mathbf{x}_N - \overline{\mathbf{x}}) - \alpha\Phi_m\Phi_m^T(\mathbf{x}_N - \overline{\mathbf{x}}). \tag{6}$$

As shown in Eq. (5), the projection is simply a weighed sum of the projections of signal and noise. On the other hand, the right-hand side of Eq. (6) contains two different terms. The first term indicates the location of a noise and the second term shows that the noise affects the entire image by the weight $-\alpha\Phi_m\Phi_m^T$. If the noise is regarded as white noise, the noise affects the image very little. On the other hand, in the case of spike noise, for example, the noise is spread over the image by the weight $-\alpha\Phi_m\Phi_m^T$.

3 Noise Region Detection/Correction

3.1 Relative Residual

Let $\mathbf{e}_j$ denote a unit vector of which the j-th element is 1 and all others are 0. Then, the relative residual $\mathbf{r}$ is defined by $\mathbf{x}^*$ and $\mathbf{x}^\sharp$ as

$$\mathbf{r}(\mathbf{x}^*, \mathbf{x}^\sharp) = \left(\frac{\mathbf{e}_1^T\mathbf{x}^\sharp}{\mathbf{e}_1^T(\overline{\mathbf{x}}+\Phi_m\mathbf{x}^*)} \quad \cdots \quad \frac{\mathbf{e}_n^T\mathbf{x}^\sharp}{\mathbf{e}_n^T(\overline{\mathbf{x}}+\Phi_m\mathbf{x}^*)} \right)^T. \tag{7}$$

We use the relative residual rather than the absolute residual ($\mathbf{x}^\natural$) for noise detection because noise should be suppressed in the relative scale, not in the absolute scale. For example, small noise in a dark area should be suppressed even if the relative residual is of sufficient size.

3.2 Noise Detection by Relative Residual

When the amount of noise is relative small compared to the signal, the distribution of the relative residual can be regarded as a zero-mean Gaussian distribution. Therefore, noise detection is basically achieved by thresholding $|\mathbf{e}_j^T \mathbf{r}|$.

On the other hand, the mean of the distribution may shift when the amount of noise increases. In order to compensate the mean shift, let us define a noise indicator $\rho_j(\mathbf{r})$ as

$$
\rho_j(\mathbf{r}) = \begin{cases} 1 & if \ |\mathbf{e}_j^T \mathbf{r} - \hat{r}| \geq r_\theta \\ 0 & otherwise \end{cases}, \quad (8)
$$

where r_θ is a threshold and $\hat{r}$ is the median of $\mathbf{e}_j^T \mathbf{r}$. In Eq. (8), the term $\rho_j(\mathbf{r})$ indicates where a considerable amount of noise is involved.

3.3 Competitive Detection of Noise Region

In general cases, the median may not be far from the mean. When multiple noise sources are included in the scene, multiple peaks may be generated and the median of the relative residual varies greatly from the mean. Furthermore, when several different signals are mixed in the scene, one signal works as noise in the other signals, and the distribution of the relative residual results in a multimodal distribution. In order to handle cases having a multimodal distribution, the noise detection method mentioned in 3.2 should be generalized.

Let $\hat{r}_k(k = 1, 2, \cdots)$ denote multiple peaks in the distribution of the relative residual. If concurrent processes are allowed for further processings, this problem is solved by replacing $\hat{r}$ with in Eq. (8) $\hat{r}_k$. In the hypothesis-and-test framework, concurrent processes will survive until a final determination is made, which selects one or more valid interpretations from among all possible interpretations.

Although the concurrent processings may cover a wider class of noise detection/correction, since the focus of the present paper is not concurrent processing, we continue our discussion by considering herein after only the single peak case.

3.4 Image Correction by Projection

When $|\mathbf{e}_j^T \mathbf{r} - \hat{r}| \geq r_\theta$, the j-th pixel of $\mathbf{x}$ is replaced by $\mathbf{e}_j^T(\overline{\mathbf{x}} + \Phi_n \mathbf{x}^*)$. The image correction causes an intensity value to be consistent with the projection. For example, the image correction causes intensities in shadow regions to become lighter, and intensities in reflection regions to become darker.

4 Optimization of Linear Projection

4.1 Simple Iterative Projection

Using the noise indicator ρ_j, we can correct a projection of $\mathbf{x}$ to the eigenspace by iterative projections. The procedure proposed in Shakunaga-Sakaue[11] is summarized as follows:

Let $\mathbf{x}_i$ denote the i-th correction of $\mathbf{x}$, where $\mathbf{x}_0$ is equivalent to $\mathbf{x}$. Define the i-th projection, residual and relative residual as

$$
\mathbf{x}_i^* = \Phi_m^T(\mathbf{x}_i - \overline{\mathbf{x}}) \quad (9)
$$
$$
\mathbf{x}_i^\natural = \mathbf{x}_0 - \overline{\mathbf{x}} - \Phi_m \mathbf{x}_i^* \quad (10)
$$
$$
\mathbf{r}_i = \mathbf{r}(\mathbf{x}_i^*, \mathbf{x}_i^\natural). \quad (11)
$$

Let us also define two diagonal matrices $\mathbf{N}_i$ and $\overline{\mathbf{N}_i}$ as

$$
\mathbf{N}_i = \mathrm{diag}(\rho_1(\mathbf{r}_i), \cdots, \rho_n(\mathbf{r}_i)) \quad (12)
$$
$$
\overline{\mathbf{N}_i} = \mathbf{I} - \mathbf{N}_i \quad (13)
$$

where $\mathbf{I}$ is a unit matrix. Then, $\mathbf{x}_{i+1} = \mathbf{X}_{i+1}/\mathbf{1}^T \mathbf{X}_{i+1}$ is given by

$$
\mathbf{X}_{i+1} = \overline{\mathbf{N}_i}\mathbf{x}_i + \mathbf{N}_i(\overline{\mathbf{x}} + \Phi_m \mathbf{x}_i^*). \quad (14)
$$

In each correction, a pixel in a noise region is replaced with the corresponding pixel in the back-projection image ($\overline{\mathbf{x}} + \Phi_m \mathbf{x}_i^*$). Because a change in $\mathbf{x}_i$ affects $\mathbf{N}_i$, we should minimize the noise effects by iterative projections. Finally, we obtain $\mathbf{x}_S$ as

$$
\mathbf{x}_S = \lim_{i \to \infty} \mathbf{x}_i. \quad (15)
$$

4.2 Optimal Projection by Linear Equations

The simple iterative projection provides a robust and effective projection. However, iterative projection often requires several iterations until convergence. In order to improve the efficiency, let us modify Eqs. (9) and (14) while taking the noise ratio α_i into account. Assume $\overline{\mathbf{N}_i}\mathbf{x}_N \approx 0$ and $\overline{\mathbf{N}_i}\mathbf{x}_S \approx \overline{\mathbf{N}_i}\mathbf{x}_i$, and let α_i denote the value of α for $\mathbf{x}_i$. The following relation is then derived from Eq. (3):

$$
\overline{\mathbf{N}_i}\mathbf{x}_0 = (1 - \alpha_i)\overline{\mathbf{N}_i}\mathbf{x}_i. \quad (16)
$$

Since $\overline{\mathbf{N}_i}\mathbf{x}_i = \overline{\mathbf{N}_i}\Phi_m \mathbf{x}_i^* + \overline{\mathbf{N}_i}\overline{\mathbf{x}}$, Eq. (16) gives

$$
\left(-\overline{\mathbf{N}_i}\Phi_m \quad \overline{\mathbf{N}_i}\mathbf{x}_0\right)\begin{pmatrix} \mathbf{x}_i^* \\ 1/(1 - \alpha_i) \end{pmatrix} = \overline{\mathbf{N}_i}\overline{\mathbf{x}}. \quad (17)
$$

Since Eq. (17) gives us simultaneous linear equations of unknown $\mathbf{x}_i^*$ and $1/(1 - \alpha_i)$, we can easily estimate $\mathbf{x}_i^*$ and α_i simultaneously. Thus, $\mathbf{x}_{i+1} = \mathbf{X}_{i+1}/\mathbf{1}^T \mathbf{X}_{i+1}$ is given by

$$
\mathbf{X}_{i+1} = \overline{\mathbf{N}_i}\mathbf{x}_0/(1 - \alpha_i) + \mathbf{N}_i(\overline{\mathbf{x}} + \Phi_m \mathbf{x}_i^*) \quad (18)
$$

and the iterative projection problem is reduced to an iterative solution of linear equations in Eq. (17), and $\mathbf{X}_{i+1}$ can be updated by Eq. (18).

4.3 Comparison

Although both the simple iterative projection and the iterative projection by linear equations provide the correct projection when noise is small, the latter method is much more efficient and slightly more robust when great deal of noise is included in the original image. The efficiency of the simple iterative projection depends on the amount of noise in the image, because each improvement is small. On the other hand, we can obtain the best possible solution by solving the linear equations. This difference results in the difference in efficiency.

5 Experimental Results

5.1 Eigenplane for Lambertian Object

In NIS, a 2-d eigenspace can be constructed for a Lambertian object. An example is shown in Fig. 1, which is constructed in NIS from eight images of a statue of Napoleon. In Fig. 1, the leftmost image is the average image, and the other images are two orthonormal bases of the eigenplane (2-d eigenspace).

Figure 1: Eigenplane for a Lambertian object.

Three examples of image correction are shown in Fig. 2. In the top and middle examples, the corrections are made around the nose. Shadow regions are detected and corrected by the proposed method. The bottom example is a case containing a great deal of noise. In the input image, a quarter of image region is covered by a black mask. In this case, we are finally able to obtain the correct signal image.
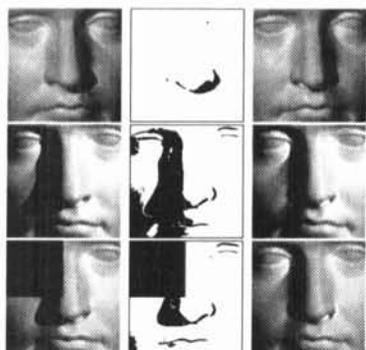
Figure 2: Image correction of a Lambertian object. Each row, from left to right, shows the original image, the detected noise and the final result are shown.

Figure 3 indicates how the iterative noise detection/correction works for the bottom example in Fig. 2. The change in distribution of the relative residual is shown in Fig. 4, where (i)-(iv) correspond to the numbers in Fig. 3. Two peaks are found in histograms (i)-(iv) in Fig. 4. In each histogram, the left-hand peak is caused by the mask region in the original image, and right-hand peak is caused by the signal. The first histogram is widely distributed around the right-hand peak. This results in incorrect detection of the noise region, as shown in Fig. 3 (ii). As the histogram becomes
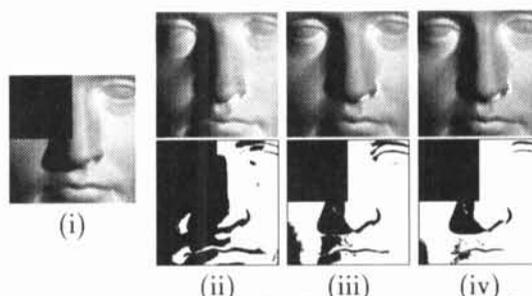
Figure 3: Sequence of projection images and noise indicators. From an original image, (i), both the projection (in the upper row) and the noise indicator (in the lower row) are gradually improved from (ii) to (iv).
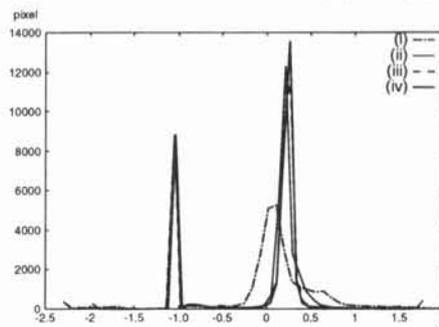
Figure 4: Change in the histogram of relative residual.

Figure 5: Eigenface for an individual.

sharp around the right-hand peak and converges, the noise region also becomes less noisy, as shown in Figs. 3 (iii) and (iv).

5.2 Individual 3-d Eigenface

The proposed method also works well for a non-Lambertian surface. An example eigenface, shown in Fig. 5, which is constructed from six individual facial images that include a little noise. Three examples of image correction are shown in Fig. 6. In the top row, the correction is performed around the nose, where the shadow region is detected and corrected. In the middle row, correction is made for the specular reflections in his glasses. In the bottom example, correction is made for an artificial noise. These examples demonstrate that the proposed method is robust to various kinds of noise, including shadows, reflections and occlusions.

5.3 Canonical 45-d Eigenface

For the class of human face, projection-based image correction still works. In this experiment, a 45-d eigenface is constructed from 50 faces, each under 20 lighting conditions. Figure 7 shows the eigenface, where the leftmost image is the average image and the other images are the most significant three bases.

Three examples of image correction are shown in Fig. 8. The target person is not included in the image set which is used for the eigenface construction. For

38
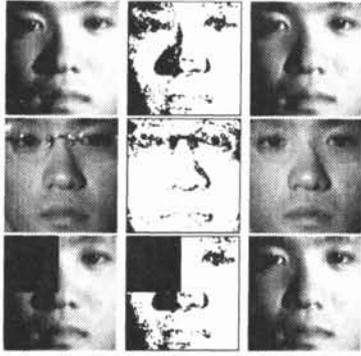
Figure 6: Noise detection/correction based on projection onto a 3-d eigenface

Figure 7: Eigenface constructed from several persons.
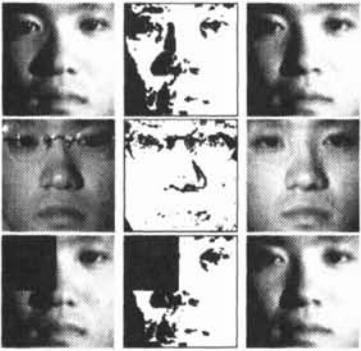
Figure 8: Noise detection/correction based on projection onto a 45-d eigenface

the comparison, all of the input images are the same images, in the same order, as those shown in Fig. 6. Experimental results in Fig. 8 show that the proposed method works well, while the result images are a little less similar to the inputs than the result in Fig. 6 because of the difference of eigenspaces. independent of the dimension of the eigenface. We have confirmed that the result images shown in Fig. 8 are a considerable improvement over those yielded by the decomposed eigenface method[10].

6   Conclusions

A projection-based image correction is discussed for a given eigenspace in NIS, and an efficient and robust implementation is provided by linear equations, as shown in Eq. (17). The improved algorithm is greatly improved in both efficiency and robustness compared to our previous implementation based on the simple iterative projection. Experimental results demonstrate that the projection-based image correction is very effective for a variety of eigenspaces, independent of the dimension of the eigenspace. The proposed method can be applied to a wide variety of computer vision techniques, including object/face recognition, tracking and computer graphics.

References

[1] Y. Adini, Y. Moses and S. Ullman, "Face recognition: The problem of compensating for changes in illumination direction," IEEE Trans. Pattern Analysis and Machine Intelligence, vol. 19, no. 7, pp. 721-732, 1997.

[2] P. N. Belhumeur, J. P. Hespanha and D. J. Kriegman, "Eigenfaces vs. Fisherfaces: Recognition Using Class Specific Linear Projection", IEEE Trans. Pattern Analysis and Machine Intelligence, vol. 19, no. 7, pp. 711-720, 1997.

[3] P. N. Belhumeur and D. J. Kriegman, "What is the set of images of an object under all possible lighting conditions?", Proc. CVPR'96, pp. 270-277, 1997.

[4] B. Moghaddam and A. Pentland, "Probabilistic Visual Learning for Object Representation", IEEE Trans. Pattern Analysis and Machine Intelligence, vol. 19, no. 7, pp. 696-710, 1997.

[5] Y. Mukaigawa, H. Miyaki, S. Mihashi and T. Shakunaga, "Photometric Image-Based Rendering for Image Generation in Arbitrary Illumination," Proc. ICCV2001, vol. 2, pp. 652-659, 2001.

[6] H. Murase and S. Nayar, "Visual Learning and Recognition of 3-d Objects from Appearance", International Journal of Computer Vision, vol. 14, pp. 5-24, 1995.

[7] K. Nishino, Y. Sato and K. Ikeuchi, "Eigen-Texture Method: Appearance Compression and Synthesis Based on a 3D Model", IEEE Trans. Pattern Analysis and Machine Intelligence, vol. 23, no. 11, pp. 1257-1265, 2001.

[8] E. Oja, Subspace Methods of Pattern Recognition, Research Studies Press Ltd., 1983.

[9] T. Shakunaga and N. Yamamoto, "Virtual Subspace Method for Robust Face Recognition Independent of Lighting Conditions", Proc. IAPR Workshop on Machine Vision Applications (MVA 2000), 2000.

[10] T. Shakunaga and K. Shigenari, "Decomposed Eigenface for Face Recognition under Various Lighting Conditions", Proc. CVPR2001, vol. 1, pp. 864-871, 2001.

[11] T. Shakunaga and F. Sakaue, "Natural Image Correction by Iterative Projections to Eigenspace Constructed in Normalized Image Space", Proc. ICPR 2002, vol. 1, pp. 648-651, 2002.

[12] A. Shashua, "Geometry and Photometry in 3D visual recognition", Ph.D. Thesis, MIT, 1992.

[13] A. Shashua and T. Riklin-Raviv, "The Quotient Images: Class-Based Re-Rendering and Recognition with Varying Illuminations", IEEE Trans. Pattern Analysis and Machine Intelligence, vol. 23, no. 2, pp. 129-139, 2001.

[14] M. Turk and A. Pentland, "Eigenfaces for Recognition", Journal of Cognitive Neuroscience, vol. 3, no. 1, pp. 71-86, 1991.

[15] A. L. Yuille, S. R. Epstein and P. N. Belhumeur, "Determining Generative Models of Objects Under Varying Illumination: Shape and Albedo from Multiple Images Using SVD and Integrability", International Journal of Computer Vision, vol. 35, no. 3, pp. 203-222, 1999.